

HEAT CAPACITIES OF

LICUCI₃ - 2H₂ 0 AND F₆CI₂ - 4H₂0

IN THE LIQUID-HELIUM
TEMPERATURE REGION

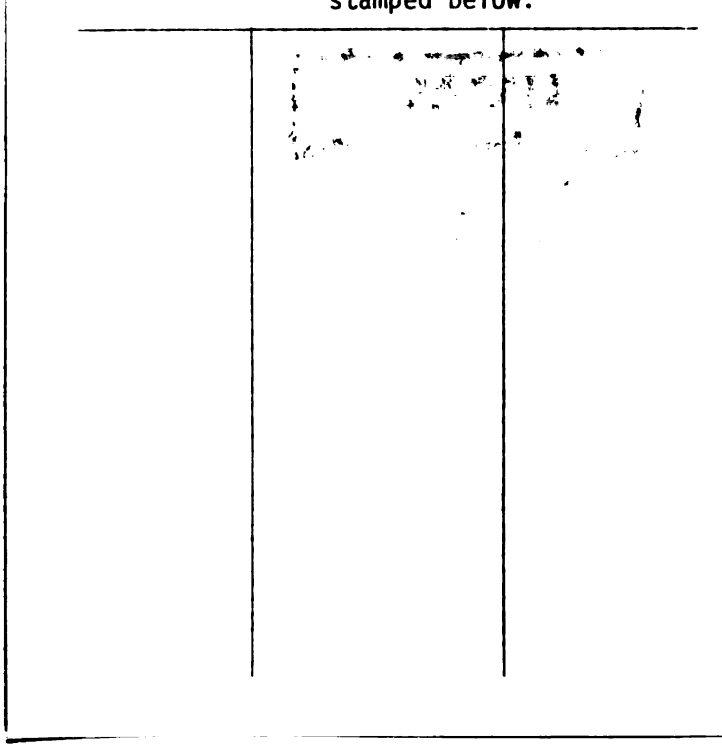
Thesis for the Degree of M. S.
MICHIGAN STATE UNIVERSITY
Donald Ray McNeeley
1961



LIBRARY Michigan State University



RETURNING MATERIALS:
Place in book drop to
remove this checkout from
your record. FINES will
be charged if book is
returned after the date
stamped below.



HEAT CAPACITIES OF LiCuCl $_3 \cdot$ 2H $_2$ O AND FeCl $_2 \cdot$ 4H $_2$ O IN THE LIQUID-HELIUM TEMPERATURE REGION

Ву

Donald Ray McNeeley

AN ABSTRACT

Submitted to
Michigan State University
in partial fulfillment of the requirements
for the degree of

MASTER OF SCIENCE

Department of Physics and Astronomy

1961

Approved fored fra.

ABSTRACT

The heat capacities of LiCuCl₃·2H₂O and FeCl₂·4H₂O have been measured in the liquid helium temperature region to determine if a λ type anomaly exists in the specific heat curve. One example of this anomaly is noted for those crystals which undergo a paramagneticantiferromagnetic transition, where it is associated with the extra energy needed to disorder the crystal. In the antiferromagnetic state the spins are aligned such that the nearest neighbors of an atom A are antiparallel to this atom. In the paramagnetic state the spins are randomly oriented.

The specific heat curve for $LiCuCl_3$ $^{\circ}2H_2O$ shows this type of anomaly at a temperature of $4.40 \pm .02^{\circ}K$. The change in magnetic entropy is also calculated for this crystal and compared with the theoretical value. In the Van Vleck theory only long-range order extending over many atomic distances is considered. However, 48% of the change in entropy occurs above the Neel temperature, indicating that a large amount of short-range order, over a few atomic distances, still persists.

The specific heat curve for FeCl₂·4H₂O shows very little temperature dependence in the region investigated, indicating perhaps that the experimental accuracy is not sufficient to disclose the expected T³ dependence of the lattice specific heat, or that this region represents the "tail" in the paramagnetic state. Such temperature independent regions have been found in other paramagnetic salts.

HEAT CAPACITIES OF LiCuCl $_3$ ·2H $_2$ O AND Fe Cl $_2$ ·4H $_2$ O IN THE LIQUID-HELIUM TEMPERATURE REGION

Ву

Donald Ray McNeeley

A THESIS

Submitted to
Michigan State University
in partial fulfillment of the requirements
for the degree of

MASTER OF SCIENCE

Department of Physics and Astronomy

ACKNOWLEDGMENTS

I would like to express my gratitude to Dr. H. Forstat who suggested the research. His continued guidance and assistance are greatly appreciated. The author also wishes to thank Sister Charles J. Zinn for help in growing the single crystals. I would like to thank the Office of Naval Research and the All-University Research Fund for financial assistance.

TABLE OF CONTENTS

	Page
THEORY	1
APPARATUS AND PROCEDURES	17
ANALYSIS OF RESULTS	28
LIST OF REFERENCES	32
APPENDIX I	34
APPENDIX II	38

LIST OF FIGURES

FIGURE	Page
1. Variation of S with y	6
2. Variation of S with T	10
3. Specific Heat of LiCuCl ₃ ·2H ₂ O	11
4. $C_p T^2 \text{ vs } T^5 \text{ for LiCuCl}_3 \cdot 2H_2O \dots$	14
5. C_p/T vs T for LiCuCl ₃ ·2H ₂ O	15
6. Heating Circuit	18
7. Thermometer and Current Controlling Circuits	20
8. Dewar System	21
9. Calorimeter	23
10. Calorimeter Vacuum System	25
ll. Specific Heat of FeCl, 4H,O	31

THEORY

In general, one defines a mean heat capacity over a temperature range T_2 to T_1 by the equation

$$\overline{C} = Q(T_2 - T_1) \tag{1}$$

The heat capacity, at any temperature T, is then defined as the limit of the above ratio when the temperature difference ΔT approaches zero, where the flow of heat is dQ:

$$C = dQ/dT (2)$$

This heat capacity is in general a function of temperature. To obtain a quantity characteristic of a substance, we define a specific heat capacity as the ratio

$$C = dq/dT (3)$$

where dq is the heat flowing into the substance per mole. As would be expected this specific heat capacity, or specific heat, depends upon the nature of the process during which heat flows into the system.

Starting with the first law of thermodynamics,

$$dQ = dU + PdV (4)$$

where U is the internal energy, P is the pressure, and V is the volume, and considering a process at constant volume, we have

$$C_{v} = (dq/dT)_{v} = (\partial U/\partial T)_{v}$$
 (5)

where we define $C_V = (\partial Q/\partial T)_V$; that is the specific heat at constant volume gives the rate of change of internal energy with respect to temperature at constant volume.

Considering a process at constant pressure,

$$(dQ/dT)_{p} = (\partial U/\partial T)_{p} + P(\partial V/\partial T)_{p}$$
 (6)

and defining

$$C_{p} = (\partial Q/\partial T)_{p} \tag{7}$$

one can see that the change in internal energy with temperature is not necessarily a simple function of the specific heat at constant pressure. It can be shown, 1 that the difference between C_p and C_v is given by,

$$C_{p} - C_{v} = B^{2}TV/k$$
 (8)

where V is the volume, B the coefficient of volume expansion, and k the compressibility. At low temperatures this difference is quite small, so that one can effectively measure C_{ν} by measuring C_{ν} .

Of interest in this paper is the temperature dependence of the specific heat of two normally paramagnetic salts. Contributions to specific heat normally arise from the lattice vibrations and the free electrons. For a paramagnetic substance, an additional magnetic contribution will be considered, due primarily to the dipole-dipole exchange interaction.

Since the crystals investigated were dielectrics, the electronic contribution was considered negligible. It can be shown² that the electronic contribution is of the form

$$C_{V} = aT$$
 (9)

where a is a constant.

For the lattice contribution, Einstein developed a simple model to account for the tendency of the lattice heat capacity to decrease at low temperatures below the value 3R per mole obtained at high temperatures, where R is the gas constant. He treated the vibrations

of the N atoms as a set of 3N independent harmonic oscillators in one dimension, each with an identical angular frequency ω . The expression for the average energy of an oscillator in quantum theory is

$$\overline{E} = \hbar \omega / (e^{\hbar \omega / kT} - 1) + \frac{1}{2} \hbar \omega$$
 (10)

At low temperatures (kt < hω), however,

$$\overline{E} = h_{\omega}e^{-\frac{h_{\omega}}{kT}} \tag{11}$$

where

$$C_{v} = Nk(-\hbar\omega/kT)^{2} e^{-\frac{\hbar\omega}{kT}}$$
 (12)

As $T\rightarrow O$ the exponential factor is dominant; yet it is found experimentally that the variation goes nearly as T^3 .

On the Einstein model each atom is assumed to be oscillating about a fixed point. Actually each oscillates relative to the other. For long wavelengths, moreover, large regions may move together. It is therefore an oversimplification to assign an identical frequency to all 3N oscillations. The long wavelength motions are particularly important at low temperatures because there will be modes of vibration for which $\hbar\omega \ll kT$. Thus some degrees of freedom will behave classically and contribute approximately kT to the energy. The total energy will not, then, approach zero exponentially.

Debye attacked the problem by ignoring the lattice structure and considering the crystal as an isotropic elastic continuum. Three modes of waves originate, two trqnsverse and one longitudinal. We find

$$v_1\lambda = v_2\lambda = C_t \tag{13}$$

and

$$v_3 \lambda = C_1$$

where ν_1 and ν_2 are the frequencies of the transverse waves, and λ is the wavelength and C_1 and C_1 are respectively the transverse and longitudinal velocities. The number of longitudinal vibrations whose frequencies lie between ν and $\nu + \Delta \nu$ is

$$4 \pi (L/C_1)^3 v^2 \Delta v$$
 (14)

where L is the length of one side of the crystal. The total number of vibrations with frequency between ν and $\nu + \Delta \nu$ is then

$$N(\nu)\Delta\nu = 4 \pi V(2/C_t^3 + 1/C_-^3) \nu^2 \Delta\nu$$
 (15)

where $L^3 = V$, the volume.

The lattice structure is taken into account by the ad hoc assumption of a cutoff frequency $\nu_{\mathbf{m}}$ such that the total number of vibrations has the correct value 3N. Then

$$3N = 4 \pi V(2/C_t^3 + 1/C^3) \int_0^{\nu_{m}} v^2 d\nu$$
 (16)

=
$$4 \pi V/3(2/C_t^3 + 1/C^3) \nu_m^3$$
 (17)

or

$$N(\nu)\Delta\nu = 9N \ \nu^2 / \nu_m^3 \ \Delta\nu \tag{18}$$

With this distribution of oscillator frequencies the average energy of the lattice is

$$\overline{E} = 9N/\nu_{m}^{3} \int_{0}^{\nu} m \left[\frac{1}{2} h\nu + \frac{h\nu}{e \frac{h\nu}{kT} - 1} \right] \nu^{2} d\nu \quad (19)$$

where $\frac{1}{2}$ h is the zero-point energy term. Using the Debye function

$$D(u) \equiv 3/u^{3} \int_{0}^{u} x^{3} dx / e^{x} - 1$$
 (20)

where

$$x \equiv h^{\nu} m / k T \equiv \theta / T \tag{21}$$

and $\theta \equiv h^{\nu}m/k$ (22)

we find
$$\overline{E} = 9/8 \text{Nh} \nu_{\text{m}} + 3 \text{NkT} \cdot D(h \nu_{\text{m}} / k T).$$
 (23)

The heat capacity at constant volume is the derivative of the energy with respect to temperature:

$$C_{x} = 3Nk \cdot D(\theta/T) + 3NkT \cdot d/dT(D(\theta/T))$$
 (24)

= 3Nk 4D(
$$\theta$$
/T) - 3(θ /T)/ e^{θ /T - 1 (25)

At low temperatures, this function reduces to

$$C_V = 3Nk \ 4 \ \pi^4/5(T/\theta)^3 + \cdots$$
 (26)

as found by experiment.

The magnetic contribution (paramagnetic), which is due to the influence of the magnetic dipole-dipole coupling and feeble exchange coupling, has been derived by VanVleck. He assumes a Hamiltonian, H, of the form

$$H = \sum_{i} v_{i} + \sum_{j>i} \omega_{ij} - H_{0} \sum_{i} \mu_{zi}$$
 (27)

with
$$\omega_{ij} = r_{ij}^{-3} \overline{\mu}_i \cdot \overline{\mu}_j - 3(\overline{\mu}_i \cdot \overline{r}_{ij}) (\overline{\mu}_j \cdot \overline{r}_{ij}) + v_{ij}^{ex}$$
 (28)

Here r_{ij} is the radius vector connecting atoms i and j, H_0 is the applied field directed along the z axis, and the μ 's are the magnetic moments of the atoms. The first part of the ω_{ij} is the dipole-dipole coupling of atoms i and j, and the last term is the exchange energy. It can be shown that

$$V_{ij}^{ex} = v_{ij} \overline{\mu_i} \cdot \overline{\mu_j} / r_{ij}^3$$
 (29)

where
$$v_{ij} = (2r_{ij}^3/g^2\beta^2) \int \frac{J(J+1) + S(S+1) - L(L+1)}{2J(J+1)} ds^2 K$$
 (30)

Here S, L, J are respectively the spin, azimuthal, and inner quantum numbers of an atom. The factor $r_{ij}^3/g^2\beta^2$ is included to make v_{ij} dimensionless. The exchange effect is then isotropic since it depends only on the relative orientation of $\overline{\mu}_i$ and $\overline{\mu}_j$. K is the exchange integral.

By expanding the partition function

$$Z \equiv \Sigma_{\lambda} e^{-W_{\lambda}} / kT$$
 (31)

where the sum is over all the states of the crystal and W $_{\chi}$ are the characteristic values of the Hamiltonian; and using

$$C_{v} = \frac{\partial}{\partial T} \left\{ kT^{2} \frac{\partial}{\partial T} \left(\log Z \right) \right\}$$
 (32)

VanVleck obtains

$$C_{v} = Nk \left[a'(\tau/T)^{2} - b'(\tau/T)^{3} - c'(\tau/T)^{4} + ...\right]$$
 (33)

where τ is defined by

$$\gamma \equiv g^2 \beta^2 N J (J+1)/k, \qquad (34)$$

and the constants a', b', c' depend upon the structure of the crystal.

At low temperatures, a reasonable approximation is given by

$$C_{v} = a/T^{2}. (35)$$

If we add to a paramagnetic substance an interaction tending to align the atomic spins in a staggered parallel arrangement we may have an antiferromagnetic media. To illustrate, consider a simple cubic or a body-centered cubic arrangement. Suppose the crystal consists of two interpenetrating sublattices such that the nearest neighbors of an atom on lattice A are entirely on lattice B. If then the spins on A are parallel in one direction and those on B in the opposite direction we have an antiferromagnetic media. For more complex arrangements additional sublattices will be needed.

It can be shown that exchange interactions are equivalent to an interatomic potential

$$V_{ij} = -\frac{1}{2}K(1 + 4\overline{S}_i \cdot \overline{S}_j)$$
 (36)

where S_i and S_j are respectively the spin angular-momentum vectors of atoms i and j in units of $h/2\pi$ and K is again the exchange integral. If K is negative, we have an antiferromagnetic media. The effective potential on a given atom i is then found by summing over the j nearest neighbors. This procedure is equivalent to saying that each atom i lies

in an effective molecular field due to atoms j. Thus except for an additive constant,

$$V_{ij} = -2K\overline{S}_{i} \cdot \Sigma \overline{S}_{j} = -2zK\overline{S}_{i} \cdot \overline{S}_{j}$$
 (37)

where z is the number of nearest neighbors of a given atom. The neighboring atoms have the same alignment, so that we have simply the product of the mean value for any one atom j and the number of such atoms z. The mean value of the spins on lattice i and j will be equal but oppositely directed. We call this value of the spin \overline{S}_0 . Hence

$$V = -2KZ\overline{S}_0^2 . (38)$$

The magnetic energy is then

$$E_{ex} = -NZ|K|\overline{S}_0^2 \tag{39}$$

where N is the number of magnetic ions per unit volume.

VanVleck⁴ has calculated the value of \overline{S}_0 . He introduces an applied field \overline{H} which produces a displacement $\delta \overline{S}_i$ and $\delta \overline{S}_j$ to the spin of typical atoms. Noting that besides the effective potential we have terms like $-g\beta \overline{S}_i$. \overline{H} due to the applied field, we write an effective field \overline{H}_{eff} . By then writing the magnetic moment \overline{M} and upon isolating correspondings contributions, we have

$$|\overline{S}_0 + \delta \overline{S}| = S B_S(y^+)$$
 (40)

$$|-\overline{S}_0 + \delta \overline{S}| = S B (y^-)$$
 (41)

where

$$y = |H = \frac{\pm}{eff} |Sg^{\beta}/kT$$
 (42)

and B_s is the Brillouin function

$$B_{S}(y) = \frac{2S+1}{2S} \coth{(\frac{2Sy+y}{2S})} - \frac{1}{2S} \coth{(\frac{y}{2S})}$$
 (43)

For zero applied field

$$|\overline{S}_0| = S B_S(y_0). \tag{44}$$

$$y_0 = 2zS \mid K\overline{S}_0 \mid /kT$$
 (45)

The Néel temperature is that temperature above which equation (44) ceases to have a real non-vanishing solution for \overline{S}_0 . For small values of the argument

$$SB_{s}(y) = (1/3)(S+1)y$$
 (46)

$$|S_0| = (1/3)(S+1)2zS |KS_0| /kT_c$$
 (47)

or
$$T_C = (2/3) | K | zk^{-1}S(S+1)$$
 (48)

Looking then at the internal magnetic energy

$$E = -Nz |K| \overline{S}_0^2$$
 (49)

we have for the specific heat

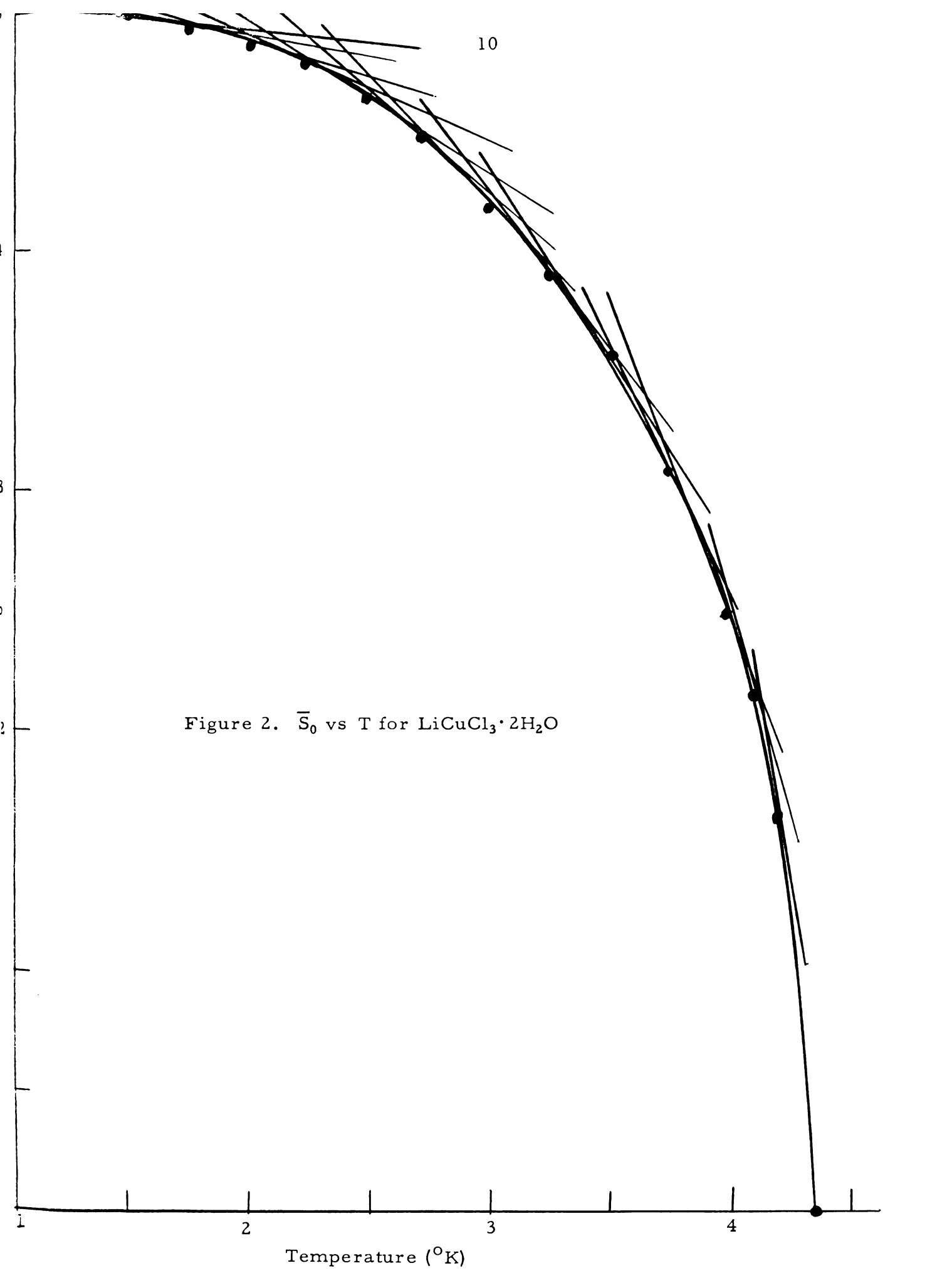
$$C_{v} = (\delta E/\delta T)_{v} = -2Nz | K| \overline{S}_{0} d\overline{S}_{0}/dT.$$
 (50)

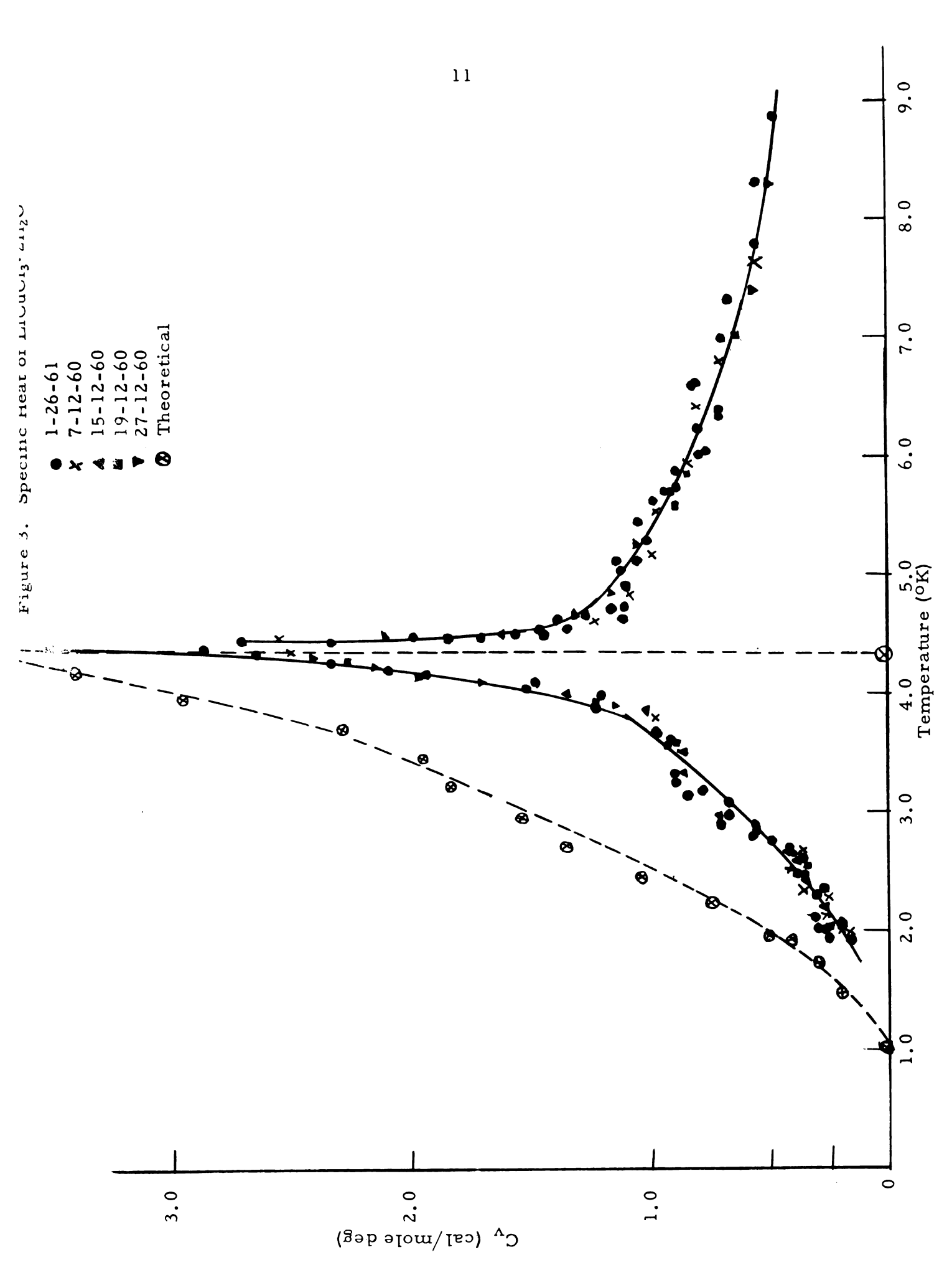
Knowing then the transition temperature and the ground state spin of the magnetic ion, we can draw the curve for C_V as a function of T. We first plot y as a function of \overline{S}_0 using equation (44). Then, using equation (45) for different values of T, we plot y as a function of \overline{S}_0 on the same graph as equation (44). These curves are shown in Figure 1. The intersection of the two curves gives a pair of \overline{S}_0 , T values. These pairs of values are then plotted in Figure 2. From this graph of \overline{S}_0 vs T, $d\overline{S}_0/dT$ values are obtained at different temperatures. These slopes are shown in Figure 2. By use of the equation for the specific heat (50) C_V values are then found for different T values, and the graph is drawn in Figure 3.

Usually a transition between different crystal modifications takes place by means of a discontinuous reconstruction of the lattice.

In addition to this crystal modification however, a transition may occur involving a change of ordering. As the temperature changes some

Figure 1. 5 vs y for LiCuCl3: 2H2O





atoms may shift relative to others. As soon as this shift begins the lattice symmetry changes. An arbitrarily small displacement is sufficient to produce an abrupt change in the symmetry of the lattice. The arrangement of the atoms in the crystal however changes continuously. A transition of this kind is called a second-order phase transition.

The transitions considered in this paper are changes in the magnetic ordering which occur at the Néel point, that is, the transitions from the antigerromagnetic to the paramagnetic state.

At absolute zero the system is completely ordered. It becomes less ordered as the temperature is increased, until the transition temperature (Néel point) is reached. Above this point the long-range order over many atomic distances disappears. However some short-range order, or correlation among near neighbors, may persist above the transition.

The Néel point may be found from an analysis of the specific heat, which has an anomaly there. This anomaly is associated with the extra internal energy required to disorder the structure. This phenomenon may be seen for LiCuCl₃·2H₂O in Figure 3.

If one divides the heat added to a system dQ by the temperature T, one gets an exact differential dS of some function of the system S called the entropy.

With this definition of entropy

$$dQ/T = dS (51)$$

we write

$$\int_{1}^{2} dQ/dT = \int_{1}^{2} dS = S_{2}-S_{1}$$
 (52)

where 1 and 2 designate the states of the system, and S_2 - S_1 designates the change in entropy.

It is then of interest to calculate the change in entropy associated with the diminution of long-range order (antiferromagnetic state) and

the change associated with short-range order (paramagnetic state).

One method for doing this is one described by Friedberg.⁵

We can calculate the change in entropy by remembering that

$$dQ = C_V dT (53)$$

Then

$$\Delta S = \int_{T_1}^{T_2} (C_{V}/T) dT$$
 (54)

This equation may be applied directly to find the change in entropy above the Néel point. We recall

$$C_v = (a/T^2) + bT^3$$
 (55)

where the electronic term has been omitted. To evaluate the constants a and b, C_VT^2 is plotted as a function of T^5 . This curve is shown in Figure 4. The slope and intercept of this curve are determined from Figure 4, and they represent the constants b and a respectively. It is found that b is so small that the lattice contribution may be neglected. Then

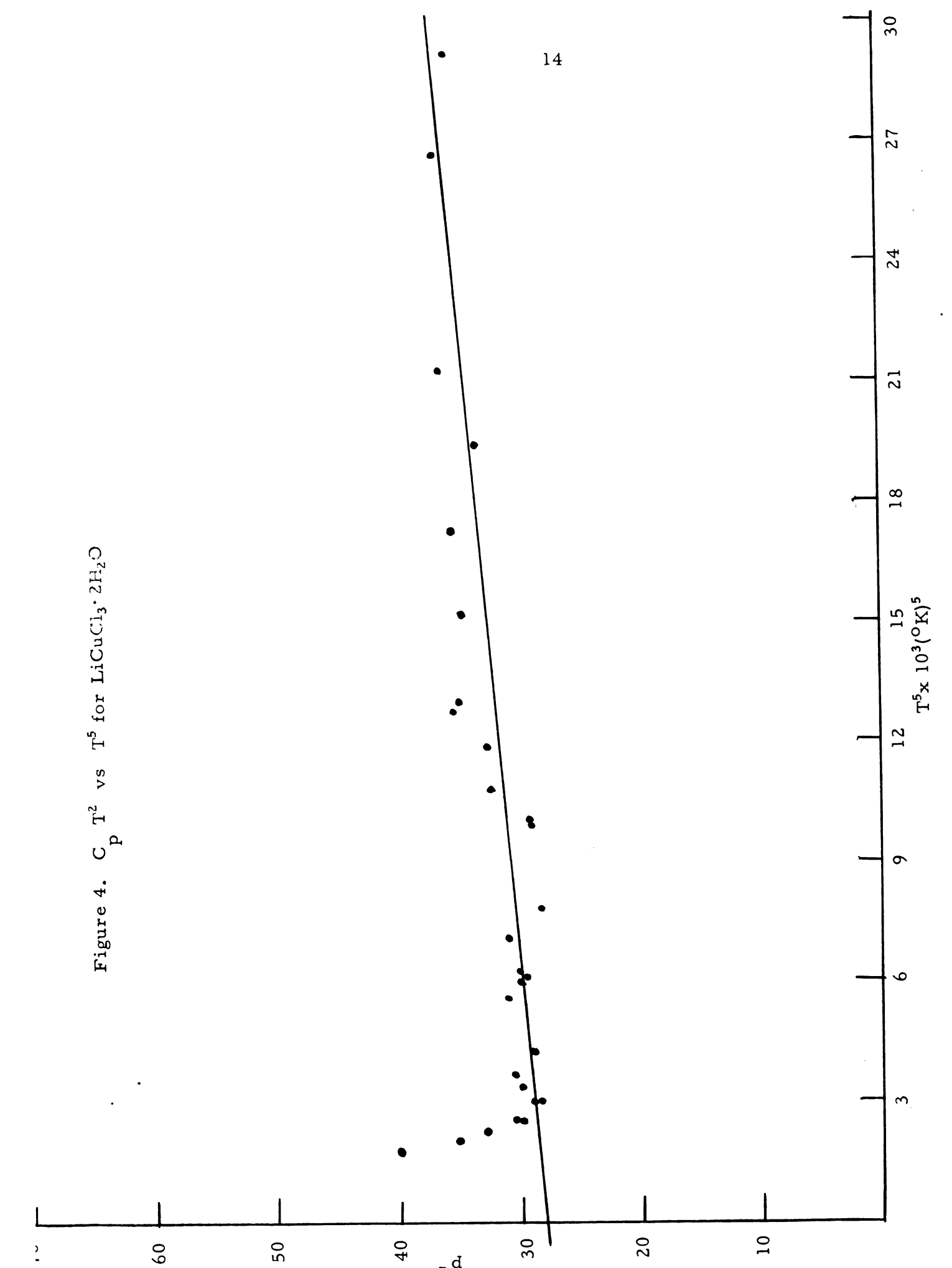
$$\Delta S = \int_{T_1}^{\infty} a/T^3 . dT$$
 (56)

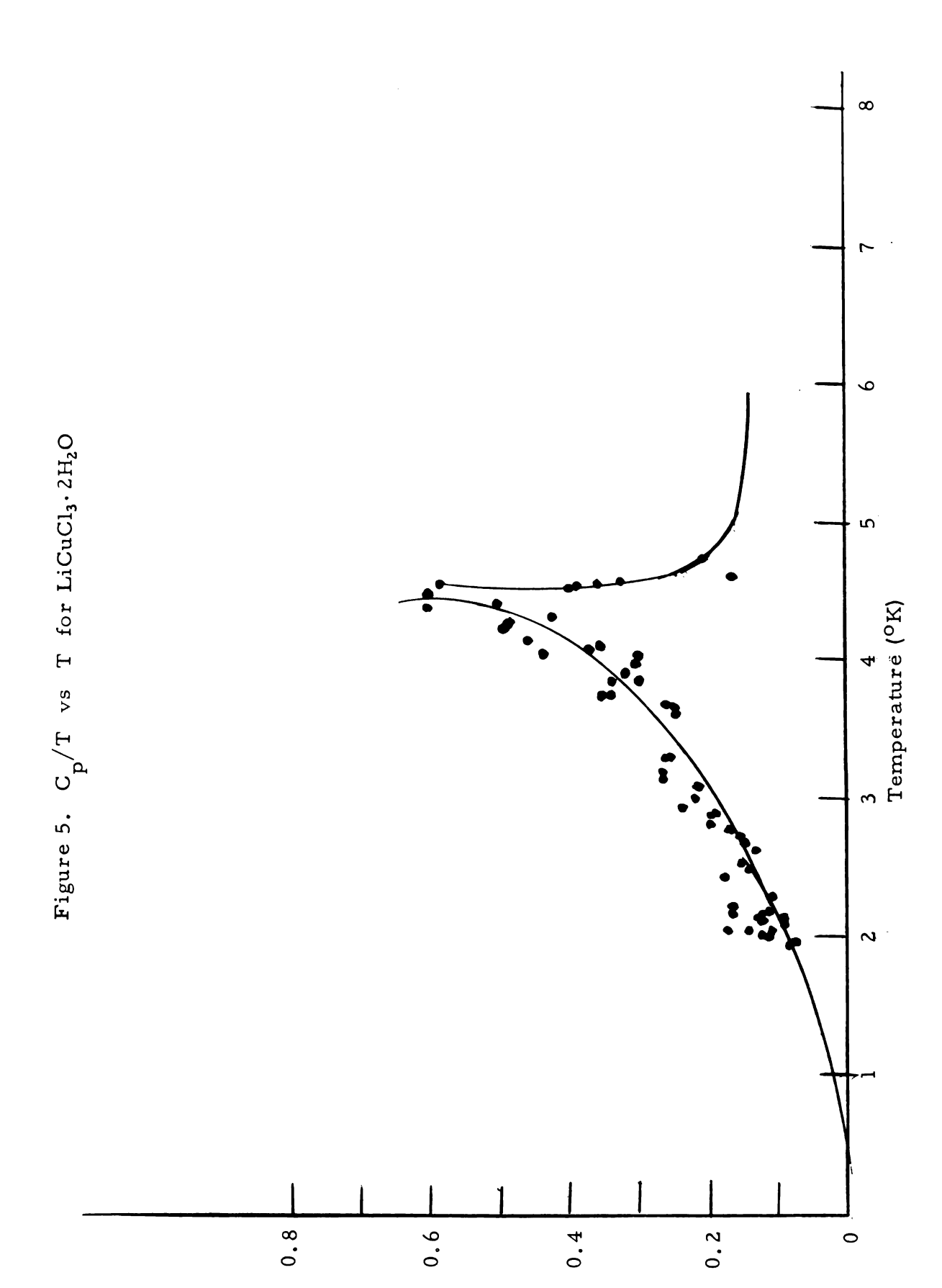
where T_1 is the temperature at which the above curve deviates from linearity. The upper limit has been extended to infinity without serious error, since the integrated function is decreasing as $1/T^2$.

For the change in entropy below the Néel point one must use a different procedure, since the specific heat is not known as an analytic function of temperature. A plot is made of $C_{\rm V}/T$ as a function of T, and the area under the curve from T=O to T=T₁ is found by graphical means. The curve of $C_{\rm V}/T$ vs T is done in Figure 5.

The total entropy change i.e., the sum of the contribution above and below the Néel temperature, may then be compared with the theoretical value of

$$\Delta S = R \log (2s+1) \tag{57}$$





where s is the ground state spin of the magnetic ion, and R is the gas constant.

The present experiment thus concerns itself first with comparing equation (50) with the experimental specific heat curve for one paramagnetic salt, and secondly with comparing the expected entropy change equation (57) with that calculated from the specific-heat data. In addition, data are also given for a paramagnetic salt that does not become antiferromagnetic in the region investigated.

APPARATUS AND PROCEDURES

In the determination of specific heat one must measure the amount of heat added to the sample, and the corresponding temperature change. For small temperature changes no appreciable error is introduced by taking the true specific heat as the specific heat at the average temperature, i.e., the average of the before-heating temperature and the after-heating temperature.

The heating circuit is shown in Figure 6. Heat is introduced into the system by passing a current through a manganin wire of approximately 400 ohms resistance at room temperature. This heating wire is wound around the crystal, and is held in place by a small amount of Glyptal. The current through this wire is measured by the potential drop across a 100 ohms standard resistance with a Leeds and Northrup type K potentiometer. By use of a reversing switch the potentiometer also measures the potential drop across the heater wire. The time during which the heat flows into the system is measured with a hand-operated stop watch accurate to 0.1 sec. The time intervals varied from 20 to 60 sec.

To measure the absolute temperature T, Allen-Bradley 0.1 watt carbon resistors were used. These resistors had a resistance of 56 ohms at room temperature, increasing to 70 ohms at liquid-air temperatures, to 500 ohms at the boiling point of liquid helium, and to 10,000 ohms at 1.3° K. These resistors show a linear relationship for $Log_{10}R$ plotted against 1/T, the line breaking at the λ point (2.18).

To determine the resistance of the thermometer, a Leeds and Northrup type k-3 potentiometer measured the potential across the thermometer. The current through the thermometer was held at

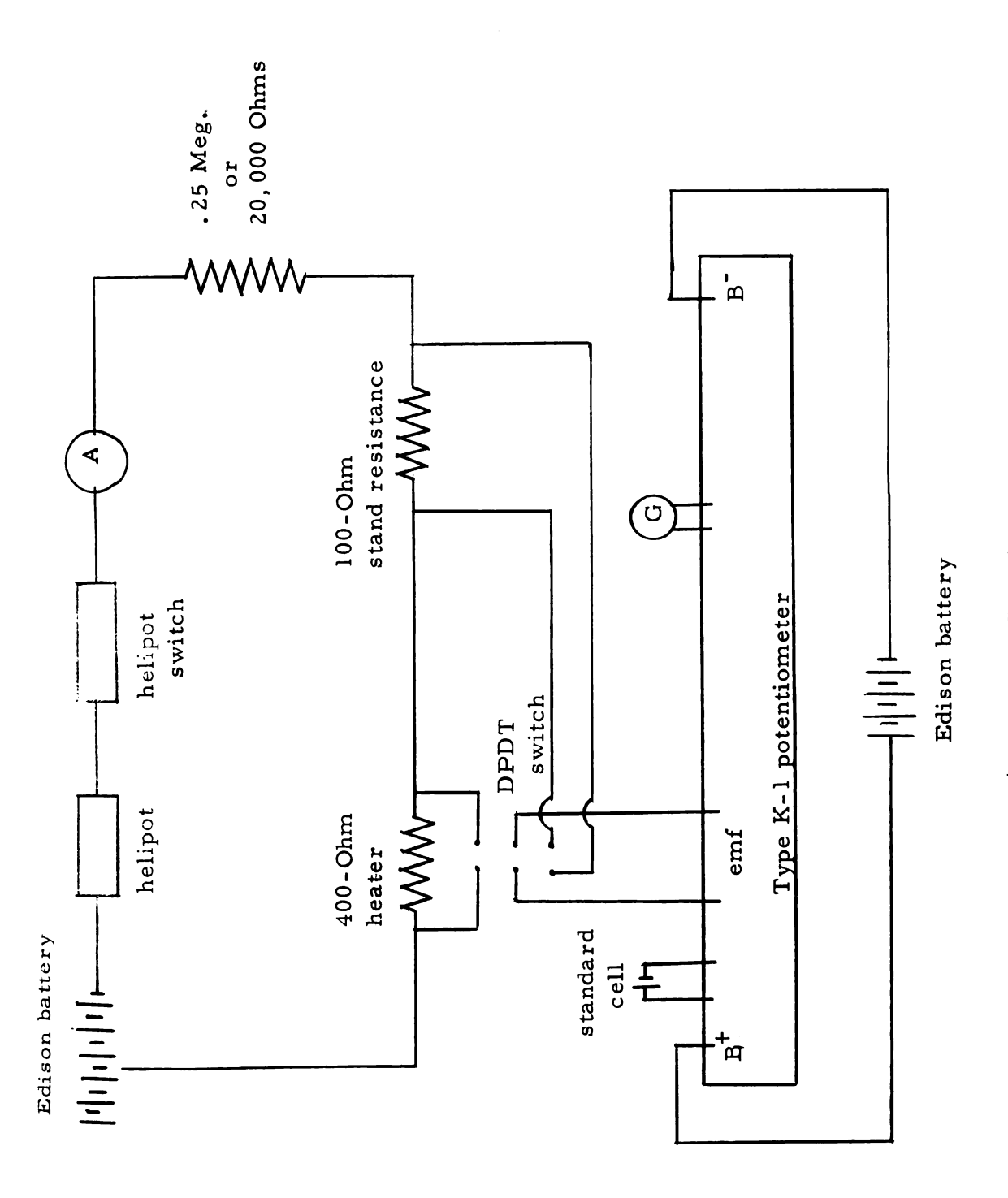


Figure 6. Heating Circuit.

10 microamperes. This was done by adjusting the current in this thermometer circuit with a 100k helipot. This adjustment was made to keep the potential drop across a 1000 ohm standard resistance in this same circuit at 10^{-2} volts as read by a Leeds and Northrup type K-2 potentiometer. This circuit is shown as the lower half of Figure 7.

The resistance of the thermometer varied continuously, however owing to the small heat leak into the system. This resultant temperature increase gave rise to an unbalance in the potentiometer. This unbalance was amplified by a Leeds and Northrup D.C. amplifier and recorded on a Leeds and Northrup Speedomax recorder. The recorder was calibrated for different voltage ranges so that, by measuring the unbalance on the chart the reading could be converted to a potential difference. By recording the potential for a balanced position, the potential at any other point could be obtained. By knowing the current through the thermometerit was now possible to determine the resistance, and consequently the temperature. The circuit used for measuring the thermometer resistance is shown as the upper half of Figure 7.

The measurements were carried out in the double-Dewar system shown in Figure 8. This system consisted of two pyrex Dewars of double wall construction. The inner Dewar, containing the helium, had a 1/4 inch glass flange attached to it. By means of a split ring below this flange and a brass T above, fastened together with eight 1/4-inch bolts, the Dewar could be sealed for reducing the vapor pressure. It had an overall length of 36 1/4 inches with a 2-inch inside and 3-inch outside diameter, with strip silvering, 1/2-inch wide. The space between the walls of the helium Dewar was first evacuated and then filled with dry nitrogen to a pressure of 1mm Hg. This space had to be reevacuated and again filled with nitrogen periodically because of the diffusion of helium gas through the Pyrex wall. At liquid-air temperatures the nitrogen gas acted as a good exchange medium.

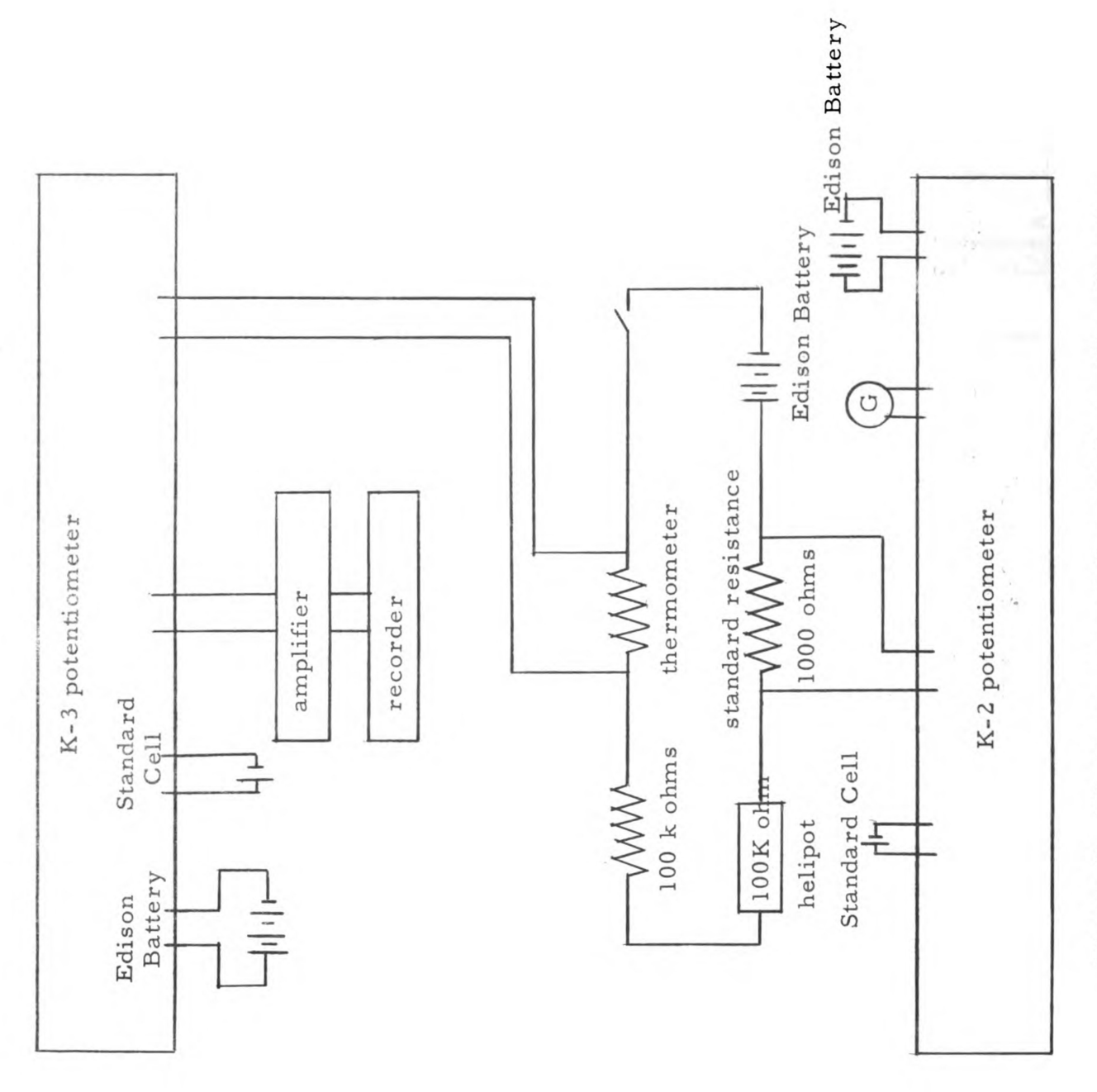


Figure 7. Thermometer and Current Controlling Circuits.

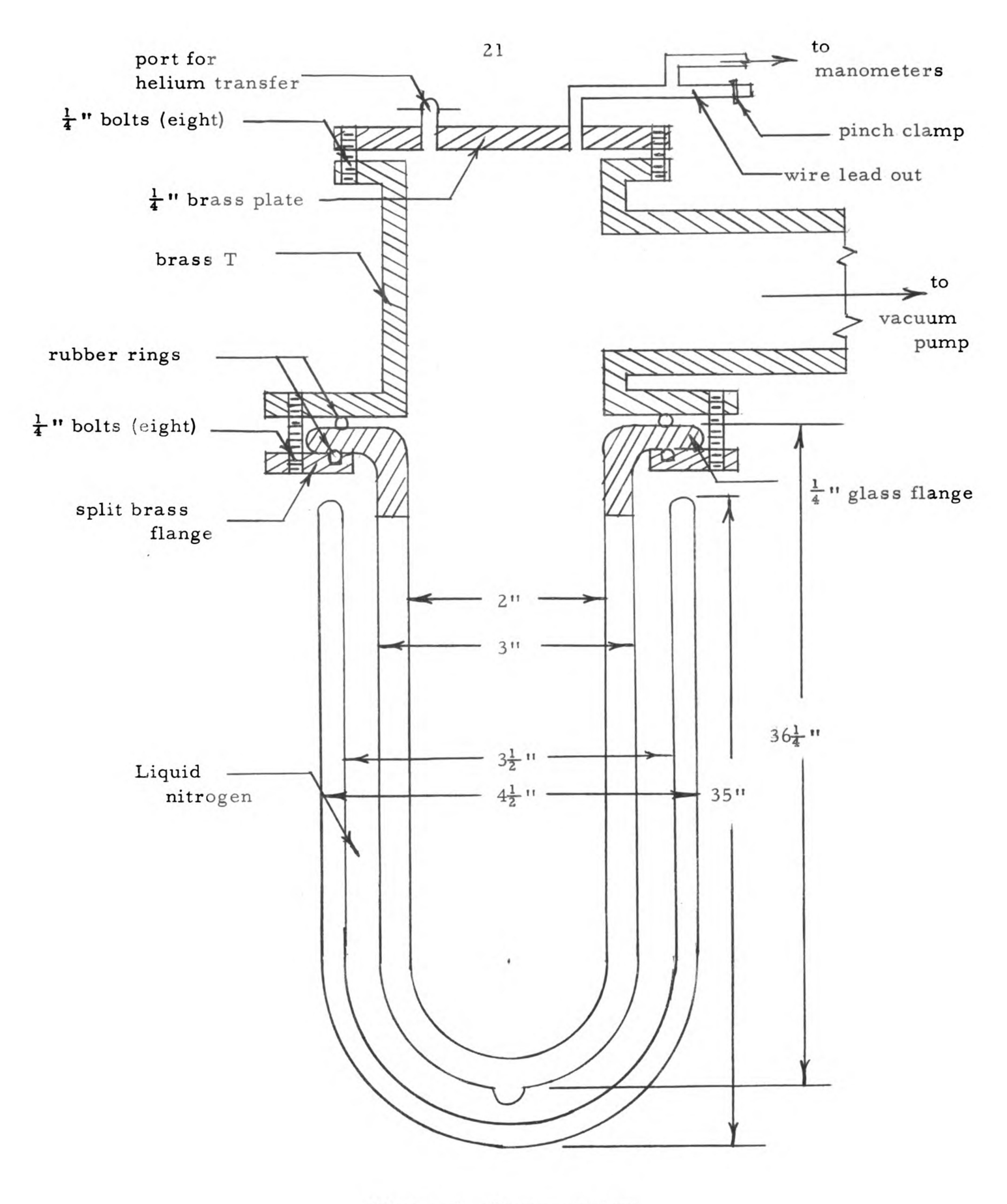


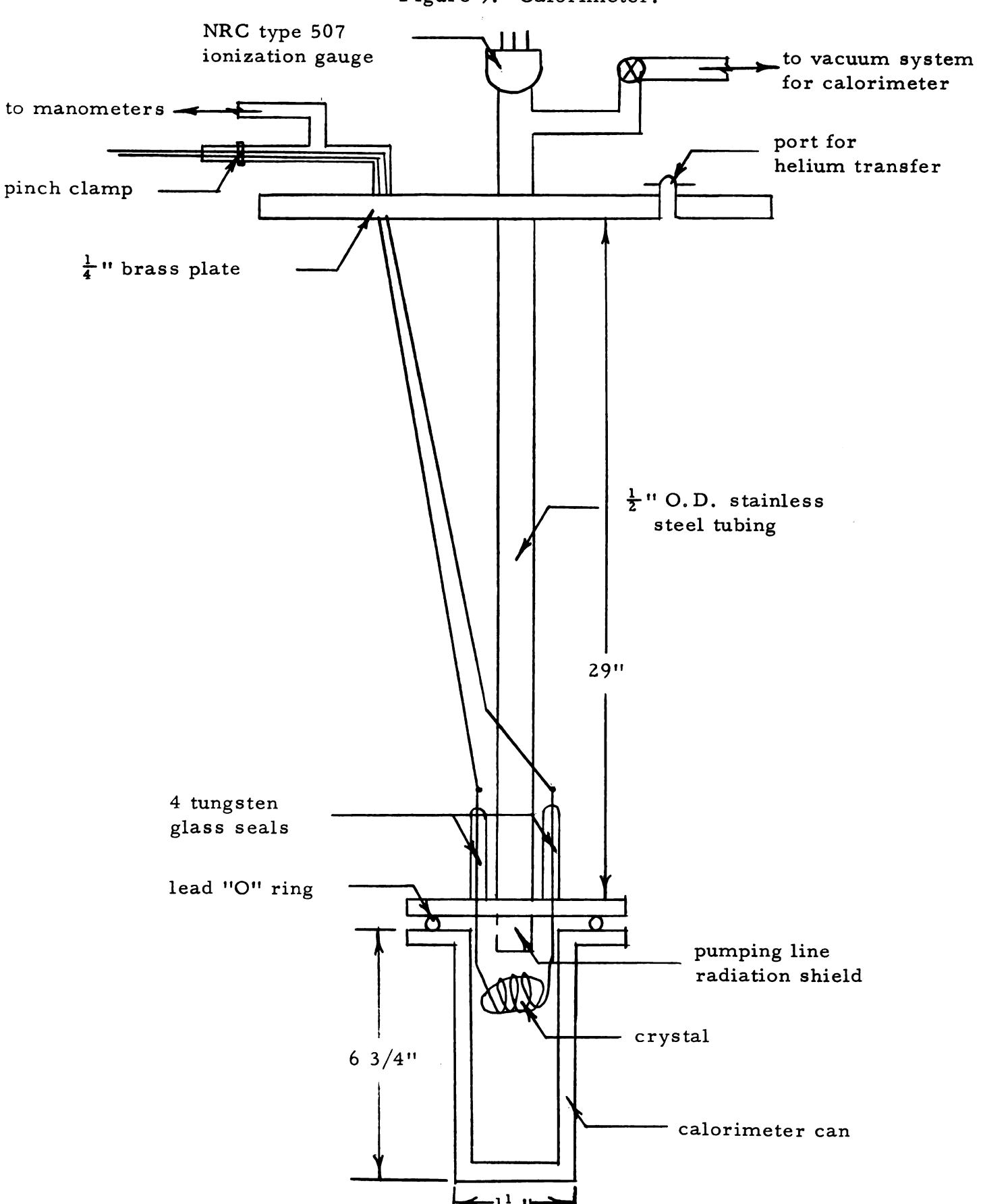
Figure 8. Dewar system.

After liquid helium was transferred into the Dewar, however, the nitrogen was frozen out, and therefore a good vacuum was obtained for isolating the helium bath from the liquid-air bath. The outer Dewar containing liquid-air, had an overall length of 35 inches with a 3 1/2-inch inside and 4 1/2-inch outside diameter, with strip silvering 1/2-inch wide.

The temperature region of interest was from $1.3^{\circ} K$ to $10^{\circ} K$. This range was obtained by controlling the vapor pressure, and by heating. For temperatures below $4.2^{\circ} K$ to the λ point, the vapor pressure was reduced with a Kinney KDH 130 vacuum pump. Below the λ point, a combination of pumping and heating was used. For temperatures above $4.2^{\circ} K$ the pressure was allowed to build up in the system to approximately two atmospheres. Because of the time for the crystal to react to a change in the temperature of the bath, its temperature could be increased above $4.2^{\circ} K$ by allowing the pressure of the bath to increase above atmospheric pressure. A second method for increasing the temperature was to bring a heating element near the Dewar system. This method however had the disadvantage of reducing the liquid helium level to a point where only one run could be made through the interval $4.2^{\circ} K$ to $10^{\circ} K$.

The calorimeter is shown in Figure 9. The calorimeter can was made of copper, 6 3/4 inches long and 1 3/8 inches in diameter. The top plate, of 1/4-inch brass, was held to the can by eight 6/32 inch screws. To obtain a vacuum seal between the two, a fuse wire "O"-ring slightly greased with Dow-Corning silicone vacuum grease was set in a groove in the top plate, which was then tightened down. The leads from the crystal were brought out of the calorimeter can through this top plate through tungsten-glass seals. To the top plate was attached a 1/2 inch O.D. stainless steel tube for evacuating the calorimeter. This tube passed up through the helium bath and was soldered at the top of the Dewar to a 1/4-inch brass plate. This plate was fastened by

Figure 9. Calorimeter.



eight 1/4-inch bolts to the top of the T, previously described, which was connected to the helium Dewar. Also in this plate was a lead-out for all wires, and a connection for the manometers. A third opening in this plate was for the transfer of liquid helium. For measuring the pressure in the calorimeter, an NRC type-507 ionization gauge was connected to the 1/2-inch tubing above the brass plate. The calorimeter was evacuated with the vacuum system shown in Figure 10.

During the course of a run the thermometer first had to be calibrated by making resistance measurements at various temperatures and plotting $\log_{10}R$ against 1/T. The vapor pressure was reduced by the pumping system already described, and the pressure was read on a mercury manometer. Below the λ -point an oil manometer was used. The density of the oil was 1/14.08 that of mercury. By using the 1958 vapor pressure versus temperature, pressure readings were converted to temperatures. From ten to fifteen calibration points were usually taken from $4.2^{\circ}K$ to $1.3^{\circ}K$. For temperatures above $4.2^{\circ}K$, extrapolation was necessary.

Following the calibration, the calorimeter was evacuated. Some heat leaks still occurred but they were of constant magnitude. To compensate for these heat leaks during a heating cycle the before and after-drifts were extrapolated to the midpoint of the heating curve. The fore-drift of the heating curve was always begun at a known value of the potential, so that by use of the recorder calibration, the potential and hence the temperature could be found at the two points on the heating curve.

By use of the data from the heating circuit and the equation

$$C_{v} = \frac{VIt}{T_{f} - T_{i}}$$
 (58)

the heat capacity at the average temperature $(T_{\rm f} - T_{\rm i})/2$ could be found.

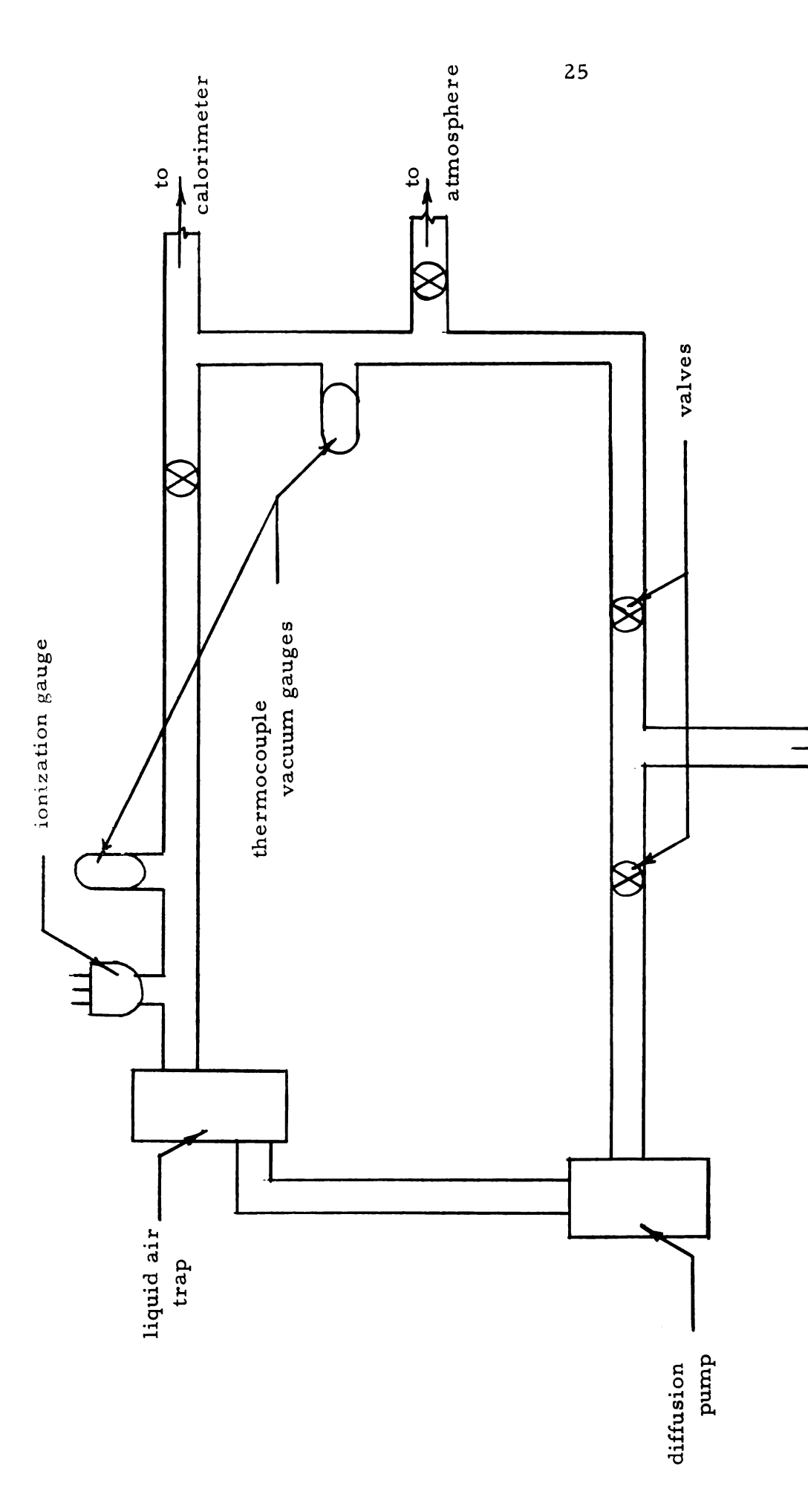


Figure 10. Calorimeter Vacuum System.

to vacuum pump

Here

V = potential across the heater
I = current through the heater
t = time of heating

 T_i and T_f = initial and final temperatures (Note: In an actual run, the specimen is maintained at constant pressure, but at low temperatures $C_p = C_v$.)

To recapitulate, the experimental data were taken as follows:

1. Precooling:

After mounting the calorimeter in the Dewar, the Dewar was flushed out with helium gas and one atmosphere of gas left in.

The liquid-air Dewar was then filled and the system was left to cool down (usually overnight). It was possible to determine when the system had reached liquid-air temperature by noting the value of the thermometer resistance.

2. Transfer:

The calorimeter was flushed out with helium and one mm Hg of helium was left in as exchange gas. Liquid helium is then transfered into the helium Dewar from the storage container by use of compressed helium gas to force it through the transfer tube.

3. Calibration:

The potential drop across the thermometer was read after it had reached equilibrium at the boiling point of liquid helium. By pumping, the vapor pressure and the temperature were lowered.

4. Isolating the system and taking of data:

After the lowest temperature had been reached the calorimeter was evacuated to remove the exchange gas and thus isolate the calorimeter from the liquid helium bath. At intervals of 3 to 5 minutes, heat was allowed to flow into the system.

Measurements of the current, potential drop, and time were taken for the heating circuit. The current and potential drop across the thermometer had been read a short time previously to give a reference point and to permit determination of the before-drift background.

Single crystals were grown from aqueous solutions at room temperature, the LiCuCl₃·2H₂O from an aqueous solution of CuCl₂·2H₂O and LiCl, and the FeCl₂·4H₂O crystals from an aqueous solution of FeCl₂·4H₂O. These salts were reagent grade, obtained from J. T. Baker Chemical Company. The LiCuCL₃.2H₂O crystals were reddish-brown, the FeCl₂·4H₂O crystals were dark green. Both types of crystals were monoclinic. All the crystals weighed 1.0 to 1.5 gm and measured approximately 1.5 x 1.0 cm. A chemical analysis was made on one of the LiCuCl₃·2H₂O crystals to verify its composition.

^{*}Analysis performed by Schwarzkopf Microanalytical Laboratory, Woodside, N. Y.

ANALYSIS OF RESULTS

LiCuCl₃· 2H₂O

Only the LiCuCl₃· 2H₂O crystal showed an anomaly in the specific heat curve in the liquid-helium temperature range. Three crystals were studied in the investigations, the third of which was also used for some nuclear magnetic resonance measurements. This nuclear-resonance data further identified the transition as paramagneticantiferromagnetic.

The specific heat curve, Figure 3, rises from about 0.25 cal/moledeg to 1.25 cal/mole-deg in the temperature range from $2-4^{\circ}K$, but increases rapidly within $0.5^{\circ}K$ from 1.25 cal/mole-deg to 3.50 cal/mole-deg (near the transition temperature). The curve then falls to approximately 1.50 cal/mole-deg at $9^{\circ}K$. This decrease follows approximately a $1/T^2$ law. The experimental data for this crystal are given in Appendix I.

The transition temperature was estimated to be $4.40 \pm .02^{\circ}$ K. This value agrees well with the nuclear resonance data, but is lower than that derived from the susceptibility measurements of Vossos, Jennings, and Rundle. ¹⁰

A comparison of the theoretical and experimental curves should be made. Below the transition point the experimental values are lower than the theoretical. The experimental curve also exhibits a tail above the transition, whereas VanVlecks' theoretical curve goes to zero. One reason for this difference is VanVleck considered only long-range ordering which goes to zero at the Néel point. However as can be seen some short-range ordering still persists above the Néel point. For the change in magnetic entropy associated with a paramagnetic-antiferromagnetic transition above the Néel temperature one must evaluate the integral

$$\Delta S = \int_{T_1}^{\infty} \frac{a}{T^3} dT$$
 (59)

From the graph of $C_p T^2 vs T^5$ in Figure 4 we obtain $T_1 = 4.57$ and a = 27.2. Thus

$$\Delta S = \int_{4.57}^{20} \frac{27.2}{T^3 dT} = 0.65 \text{ cal/mole-deg}$$
 (60)

The change in entropy below the Néel point is found by graphically measuring the area under the curbe of C_p/T vs T from 0° -4.57°K, in Figure 5. The entropy change in the region 0° -4.57°K, is calculated to be 0.70 cal/mole-deg. The total change in entropy is therefore 1.35 cal/mole-deg. We wish to compare this total entropy change with the theoretical equation (57). The exact composition of the magnetic ion is unknown. However if one assumes a spin of $\frac{1}{2}$ for the copper (possibly as $CuCl_3$) then the theoretical change in magnetic entropy is 1.38 cal/mole-deg, a value within 2% of that obtained experimentally. However, in the susceptibility measurements 10 it is found that a better fit to the data is obtained if s is taken as 1 for copper (as Cu_2Cl_6). A more detailed examination of this point must await neutron-diffraction experiments.

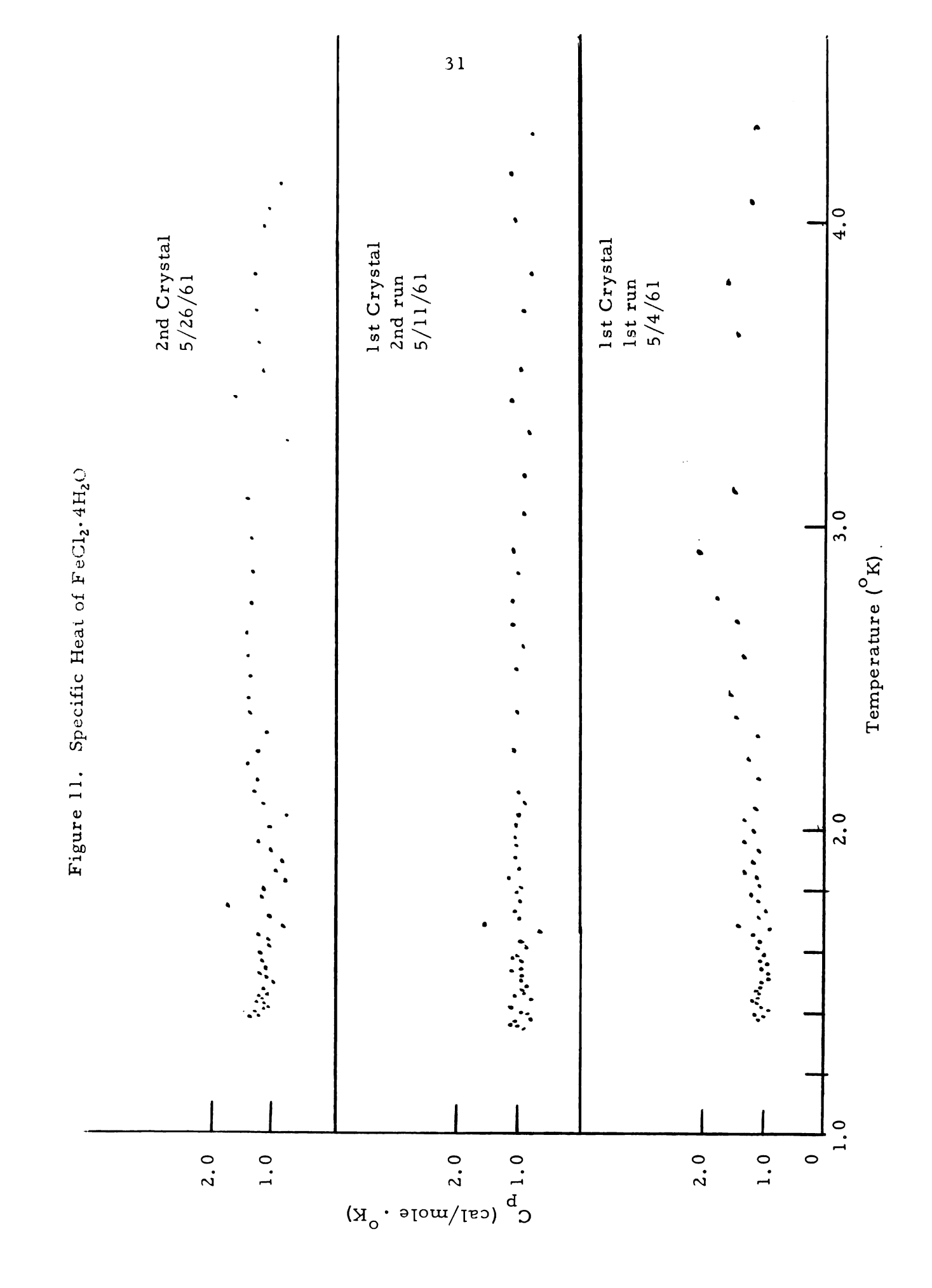
It should also be noted that 48% of the change in entropy occurs above the Néel temperature. This entropy change is associated with the diminution of short-range order, a phenomenon neglected in VanVleck's simple model. Such a large fraction has also been observed in a number of other antiferromagnets.

FeCl₂·4H₂O

In the case of FeCl₂·4H₂O no transition was found in the temperature region investigated. Neutron-diffraction investigations by Wilkinson and

Cable¹¹ on polycrystalline samples of anhydrous FeCl₂ from 4.2°K to room temperature indicate an antiferromagnetic-paramagnetic transition at 24°K. From previous work by other investigators on the anhydrous and hydrated forms of paramagnetic crystals, it was shown that in a number of cases, if the anhydrous form of the paramagnetic crystal became antiferromagnetic, then the hydrated form showed an antiferromagnetic state at a lower temperature. From this fact the present investigator felt that a magnetic transition might be observed in the helium region with a hydrated sample of FeCl₂. Apparently however the tetrahydrate of FeCl₂ is magnetically too dilute to show such a transition in this region. Possibly FeCl₂·4H₂O is antiferromagnetic at a temperature not attainable with the present pumping system.

Figure 11 shows the specific heat curves obtained for FeCl₂·4H₂O in three separate runs on two different crystals. The specific heat values are quite small, and appear to remain constant over the temperature range investigated. From the experimental data no T³ dependence of the heat capacity is observed. It is possible that this is due to the lack of experimental accuracy. On the other hand, this heat capacity data may be in a region corresponding to the "tail" in an antiferromagnetic-paramagnetic transition. This has been observed previously in MnCl₂·4H₂O. ¹² That this data does represent such a region is not too unreasonable, since it has been reported previously that FeCl₂·4H₂O shows a magnetic transition at approximately 1.6°K. ¹³ Further work at lower temperatures will help to clarify this point. The experimental data are given in Appendix II.



LIST OF REFERENCES

- 1) F. W. Sears, <u>Thermodynamics</u>, (Addison-Wesley Pub. Co. Cambridge, Mass., 1956).
- 2) C. Kittel, Introduction to Solid State Physics, (John Wiley and Sons, Inc., New York: 2nd edition, 1956).
- 3) J. H. VanVleck, J. Chem. Phys. 5, 320 (1937).
- 4) J. H. VanVleck, J. Chem. Phys. 9, 85 (1941).
- 5) S. A. Friedberg, Physica 18, 714 (1952).
- 6) J. R. Clement and E. H. Quinnell, Rev. Sci. Instr. 22, 213 (1952).
- 7) H. Forstat and J. Novak, Rev. Sci. Instr. 29, 733 (1958).
- 8) F. G. Brickwedde, H. vanDijk, M. Durieux, J. R. Clement, and J. K. Logan, J. Research (N. B.S.) 64A, 1 (1960).
- 9) R. D. Spence and C. R. K. Murty, (to be published in Physica).
- P. H. Vossos, L. D. Jennings, and R. E. Rundle, J. Chem. Phys. 32, 1590 (1960).
- 11) M. K. Wilkinson and J. W. Cable, Bull. Am. Phy. Soc. II <u>1</u>, 190 (1956).
- 12) H. Forstat, G. O. Taylor and B. R. King, J. Phys. Soc. Japan <u>15</u>, 528 (1960).
- 13) R. D. Pierce and S. A. Friedberg, J. Appl. Phys. 32, 66 (1961).

APPENDICES

APPENDIX I

Experimental Data for LiCuCl₃·2H₂O

Cn	ΔΤ	T
C _p o(cal/mole oK)	ΔT (°K)	(°K)
	7 Dec. 1960	
0.15	0.009	1.998
0.19	0.010	2.018
0.25	0.008	2.155
0.25	0.007	2.157
0.24	0.008	2.265
0.34	0.006	2.329
0.34	0.005	2.365
0.39	0.004	2.571
0.37	0.005	2.641
0.34	0.006	2.677
0.93	0.009	3.821
2.46	0.006	4.387
3.517	0.004	4.392
	15 Dec. 1960	
0.24	0.005	2.043
0.26	0.005	2.063
0.28	0.005	2.084
0.23	0.005	2.103
0.27	0.004	2.145
0.29	0.004	2.189
0.26	0.004	2.214
0.34	0.003	2.400
0.36	0.004	2.633
0.44	0.004	2.663
0.71	0.012	2.963
0.86	0.008	3.314
0.84	0.009	3.539
0.93	0.008	3.865
1.34	0.016	4.002
	19 Dec. 1960	
0.21	0.003	2.065
0.27	0.003	2.257
0.22	0.004	2.291
0.23	0.003	2.330
0.36	0.002	2.441

Continued

C _p cal/mole ^O K)	ΔΤ ([°] K)	T (°K)		
	19 Dec. 1960 (cont'd)			
0.38	0.002	2.479		
0.35	0.002	2.543		
0.33	0.003	2.621		
0.88	0.009	3.582		
1.97	0.009	4.169		
	22 Dec. 1960			
0.16	0.005	1.921		
0.18	0.004	1.938		
0.21	0.004	1.954		
0.24	0.003	2.013		
0.26	0.006	2.069		
0.24	0.003	2.098		
0.33	0.003	2.448		
0.37	0.021	2.702		
0.46	0.013	2.756		
0.50	0.011	2.819		
1.09	0.015	3.716		
2.12	0.007	4.295		
0.53	0.180	7.389		
0.49	0.204	8.259		
	26 Inn 1061			
0.17	26 Jan. 1961	1 004		
	0.004	1.904		
0.15	0.004	1.920		
0.23	0.003	1.964		
0.25	0.003	1.979		
0.24 0.004		2.016		
0.29 0.20	0.003 0.003	2.034 2.066		
0.26	0.003	2.097		
0.29	0.003	2.129		
0.26	0.003	2.146		
0.26	0.003	2.217		
0.25	0.014	2.269		
0.29	0.012	2.361		
0.35	0.009	2.470		
0.38	0.007	2.512		
0.36	0.010	2.598		
0.40	0.007	2.663		
0.41	0.007	2.703		

		
C_{p}	Δ T	T
C _p o(cal/mole K)	(°K)	(°K)
	26 Jan. 1961 (cont'd)	
0.47	0.011	2.752
0.56	0.010	2.805
0.57	0.011	2.846
0.45	0.013	2.888
0.70	0.008	2.928
0.67	0.009	2.978
0.67	0.021	3.072
0.84	0.026	3.145
0.88	0.008	3.290
0.88	0.012	3.320
0.90	0.007	3.613
0.90	0.007	3.639
0.96	0.013	3.696
1.23	0.009	3.896
1.20	0.010	3.962
1.22	0.010	4.000
1.51	0.008	4.069
1.48	0.009	4.107
1.93	0.007	4.187
2.10	0.005	4.225
2.09	0.009	4.274
2.64	0.005	4.357
2.86	0.008	4.421
2.71	0.008	4.446
1.98	0.006	4.491
1.44	0.014	4.501
1.47	0.013	4.552
1.32	0.015	4.579
1.38	0.011	4.648
1.11	0.018	4.744
1.11	0.015	4.731
1.14	0.044	4.953
1.17	0.038	5.052
1.16	0.058	5.139
1.02	0.065	5.323
1.09	0.036	5.476
0.99	0.035	5.633
0.91	0.039	5.708
0.93	0.059	5.731
0.90	0.043	5.775

continued

C _p o(cal/mole oK)	ΔΤ ([°] K)	T (°K)	
	26 Jan. 1961 (cont'd)		
0.89	0.073	5.892	
0.76	0.110	6.050	
0.81	0.071	6.632	
0.80	0.062	6.653	
0.73	0.147	6.867	
0.72	0.138	7.023	
0.67	0.146	7.340	
0.58	0.159	7.820	
0.56	0.152	8.320	
0.47	0.173	8.874	

APPENDIX II

Experimental Data FeCl₂·4H₂O

1st Crystal, 1st Run

4 May 1961

					
T	ΔΤ	С	Т	ΔΤ	С
1.3750	0.0044	1.08	1.7604	0.0034	1.06
1.3814	0.0038	1.01	1.7815	0.0045	1.20
1.3918	0.0037	1.15	1.8051	0.0049	1.08
1,4034	0.0043	0.91	1.8298	0.0114	1.11
1.4124	0.0036	1.03	1.8588	0.0099	1.32
1.4226	0.0032	1.12	1.8925	0.0100	1.15
1.4348	0.0033	1.18	1.9256	0.0097	1.07
1.4462	0.0032	1.10	1.9599	0.0077	1.32
1.4587	0.0034	1.06	1.9930	0.0092	1.18
1.4709	0.0028	1.10	2.0323	0.0144	1.33
1.4828	0.0029	1.04	2.0740	0.0176	1.13
1.4930	0.0037	1.01	2.1692	0.0160	1.06
1.5056	0.0039	0.96	2.2266	0.0169	1.26
1.5234	0.0037	0.94	2.3081	0.0112	1.62
1.5393	0.0033	1.05	2.3749	0.0107	1.46
1.5539	0.0039	0.95	2.4422	0.0137	1.53
1.5669	0.0044	1.03	2.5723	0.0126	1.37
1.5831	0.0038	1.00	2.6856	0.0195	1.42
1.5950	0.0038	1.00	2.7559	0.0144	1.80
1.6081	0.0031	1.09	2.9103	0.0135	2.10
1.6297	0.0032	1.03	3.1235	0.0186	1.49
1.6537	0.0038	1.15	3.6284	0.0289	1.45
1.6715	0.0042	0.91	3.7955	0.0231	1.62
1.6853	0.0026	1.39	4.0700	0.0298	1.27
1.7098	0.0038	1.07	4.3114	0.0502	1.63
1.7313	0.0036	0.95			
		1 - 4 C	1 2 1 D		
		-	1, 2nd Run		
		11 May	/ 1701		
1.3379	0.0015	1.41	1.7295	0.0120	1.04
1.3442	0.0024	0.94	1.7556	0.0135	0.99
1.3499	0.0022	1.02	1.7851	0.0128	1.00
1.3573	0.0020	1.13	1.8131	0.0122	0.97
1.3651	0.0019	1.07	1.8389	0.0115	1.19
1.3767	0.0025	0.82	1.8667	0.0139	1.02
1.3883	0.0023	0.86	1.9035	0.0156	1.05

continued

T	ΔΤ	Ср	T	ΔΤ	C _p	
lst Crystal, 2nd Run 11 May 1961 (cont'd)						
1.3974	0.0020	0.98	1.9395	0.0120	1.04	
1.4068	0.0031	1.11	1.9739	0.0125	1.05	
1.4182	0.0040	0.81	2.0100	0.0121	1.04	
1.4365	0.0039	1.01	2.0431	0.0138	1.01	
1.4508	0.0035	0.92	2.0799	0.0156	0.90	
1.4635	0.0038	0.95	2.1211	0.0149	1.01	
1.4772	0.0032	0.90	2.2640	0.0112	1.10	
1.4964	0.0033	0.95	2.3778	0.0209	1.05	
1.5123	0.0030	0.93	2.4704	0.0317	0.65	
1.5282	0.0025	1.12	2.5313	0.0173	1.03	
1.5449	0.0038	0.96	2.6045	0.0237	0.93	
1.5557	0.0034	0.95	2.6738	0.0200	1.11	
1.5695	0.0032	1.09	2.7480	0.0166	1.12	
1.5855	0.0030	1.02	2.8393	0.0194	1.08	
1.6097	0.0096	0.87	2.9240	0.0240	1.10	
1.6317	0.0077	0.97	3.0382	0.0212	0.95	
1.6570	0.0116	0.66	3.1731	0.0231	0.93	
1.6797	0.0048	1.58	3.2987	0.0250	0.83	
1.7041	0.0151	0.98	3.4089	0.0267	1.12	
			3.5113	0.0246	0.99	
			3.6991	0.0506	0.95	
			3.8337	0.0485	0.83	
			3.9958	0.0990	1.10	
			4.1558	0.0812	1.14	
			4.2912	0.0573	0.81	
		2nd	l Crystal			
			May 1961			
1.3678	0.0038	0.76	1.8021	0.0181	1.17	
1.3750	0.0025	1.24	1.8314	0.0144	0.81	
1.3815	0.0028	1.14	1.8632	0.0181	0.96	
1.3882	0.0021	1.31	1.8993	0.0151	0.83	
1.3951	0.0025	1.16	1.9300	0.0182	1.01	
1.4026	0.0030	1.07	1.9635	0.0146	1.22	
1.4104	0.0028	1.13	1.9984	0.0160	1.02	
1.4233	0.0024	1.29	2.0360	0.0145	0.77	
1.4294	0.0024	1.15	2.0789	0.0242	1.26	
1.4367	0.0025	1.21	2.1194	0.0212	1.30	
		- • - •		-,		

continued

T	ΔT	C _p	T	ΔT	c_p		
2nd Crystal							
			1ay 1961				
			ont'd)				
1.4530	0.0051	1.09	2.1636	0.0196	1.24		
1.4663	0.0031	1.14	2.2119	0.0195	1.39		
1.4891	0.0041	0.99	2.2609	0.0225	1.24		
1.5034	0.0048	1.11	2.3191	0.0225	1.09		
1.5178	0.0104	1.22	2.3798	0.0249	1.36		
1.5347	0.0104	1.11	2.4343	0.0202	1.39		
1.5550	0.0092	1.16	2.4978	0.0243	1.34		
1.5611	0.0084	1.19	2.5651	0.0243	1.41		
1.5878	0.0101	1.18	2.6462	0.0210	1.42		
1.6099	0.0096	1.06	2.7454	0.0234	1.37		
1.6308	0.0096	1.07	2.8467	0.0390	1.35		
1.6543	0.0170	1.20	2.9568	0.0245	1.35		
1.6803	0.0178	0.81	3.0910	0.0345	1.42		
1.7144	0.0194	1.04	3.2783	0.0946	0.76		
1.7493	0.0119	1.74	3.4162	0.0510	1.69		
1.7729	0.0160	1.19	3.5114	0.0518	1.20		
			3.6024	0.0415	1.28		
			3.7129	0.0675	1.30		
			3.8347	0.0736	1.31		
			3.9835	0.0651	1.18		
			4.0478	0.0409	1.10		
			4.1230	0.0527	0.94		
			1,1230		/ -		

MICHIGAN STATE UNIVERSITY LIBRARIES

3 1293 03145 5946